This work was partly supported by a Grant-in-Aid for Scientific Research from the Ministry of Education, Science and Culture, Japan. The cost of the high-temperature facility was partly defrayed by a grant from RCA Research Laboratories, Inc.

References

International Tables for X-ray Crystallography (1974). Vol. IV, pp. 71–151. Birmingham: Kynoch Press.

KURIHARA, T., OHASHI, Y. & SASADA, Y. (1982). *Acta Cryst.* B**38**, 2484–2486.

MAIN, P., HULL, S. E., LESSINGER, L., GERMAIN, G., DECLERCQ, J. P. & WOOLFSON, M. M. (1978). *MULTAN* 78. *A System of Computer Programs for the Automatic Solution of Crystal Structures from X-ray Diffraction Data.* Univs. of York, England, and Louvain, Belgium.

OHASHI, Y. (1975). Unpublished version of an original program by T. ASHIDA.

OHASHI, Y. & SASADA, Y. (1977*a*). *Nature (London)*, **267**, 142–144.

OHASHI, Y. & SASADA, Y. (1977*b*). *Bull. Chem. Soc. Jpn*, **50**, 2863–2869.

OHASHI, Y., SASADA, Y. & OHGO, Y. (1978*a*). *Chem. Lett.* pp. 457–460.

OHASHI, Y., SASADA, Y. & OHGO, Y. (1978*b*). *Chem. Lett.* pp. 743–746.

OHASHI, Y., UCHIDA, A., SASADA, Y. & OHGO, Y. (1983). *Acta Cryst.* B**39**, 54–61.

OHASHI, Y., YANAGI, K., KURIHARA, T., SASADA, Y. & OHGO, Y. (1981). *J. Am. Chem. Soc.* **103**, 5805–5812.

OHASHI, Y., YANAGI, K., KURIHARA, T., SASADA. Y. & OHGO, Y. (1982). *J. Am. Chem. Soc.* **104**, 6353–6359.

OHGO, Y., TAKEUCHI, S., NATORI, Y., YOSHIMURA, J., OHASHI, Y. & SASADA, Y. (1981). *Bull. Chem. Soc. Jpn*, **54**, 3095–3099.

SHELDRICK, G. M. (1976). *SHELX* 76. Program for crystal structure determination. Univ. of Cambridge, England.

Acta Cryst. (1983). B**39**, 250–257

The Molecular Symmetry of Glutaminase-Asparaginases: Rotation Function Studies of the *Pseudomonas* 7A and *Acinetobacter* Enzymes

BY HERMAN L. AMMON AND KENAN C. MURPHY

Department of Chemistry, University of Maryland, College Park, MD 20742, *USA*

LENNART SJOLIN

Laboratory of Molecular Biology, National Institute of Arthritis, Diabetes, Digestive and Kidney Diseases, Bethesda, MD 20205, *USA*

ALEXANDER WLODAWER

National Measurements Laboratory, National Bureau of Standards, Washington, DC 20234, *USA*

JOHN S. HOLCENBERG

Department of Pharmacology and Toxicology, The Medical College of Wisconsin, Milwaukee, WI 53226, *USA*

AND JOSEPH ROBERTS

Sloan-Kettering Institute for Cancer Research, Rye, NY 10580, *USA*

(*Received* 23 *February* 1982; *accepted* 22 *July* 1982)

Abstract

The molecular symmetry of crystalline *Pseudomonas* 7A glutaminase-asparaginase (orthorhombic, $P2_12_12_1$, $a = 118{\cdot}0$, $b = 131{\cdot}2$, $c = 85{\cdot}1$ Å), which contains one 139 000 g mol^{-1} tetramer per asymmetric unit, has been studied with Patterson rotation techniques. The results are completely consistent with 222 point-group symmetry. The relative orientations of the crystalline *Acinetobacter* glutaminase-asparaginase (orthorhombic, $I222$, $a = 96{\cdot}7$, $b = 112{\cdot}4$, $c = 70{\cdot}9$ Å), which contains one subunit per asymmetric unit, and the *Pseudomonas* 7A enzyme have been established with the so-called locked and cross-rotation functions. The presence of 222 symmetry in these tetramers is consistent with several previous investigations of the asparaginases.

Introduction

The administration of L-asparaginase (L-asparagine amidohydrolase, EC 3.5.1.1) produces the regression of

0567-7408/83/020250-08$01.50

certain tumors in experimental animals and in humans (Kidd, 1970). The *Escherichia coli* enzyme has been used in the treatment of acute lymphocytic leukemias for more than a decade (Oettgen, Old, Boyse, Campbell, Philips, Clarkson, Tallal, Leeper, Schwartz & Kim, 1969). The enzyme differs fundamentally from other chemotherapeutic agents used in the treatment of neoplastic disease, in that its action is based on a specific metabolic defect in certain cancer cells which is not present in normal host cells (Montgomery, 1976). Asparaginase-sensitive tumor cells have a diminished capacity to synthesize L-asparagine because of relatively low levels of the enzyme L-asparagine synthetase (Cooney, Driscol, Milman, Jayaram & Davis, 1976), resulting in the requirement for an exogenous supply of the amino acid.

L-Glutamine, like L-asparagine, is not an essential component in the human diet. The amino acid is involved in a variety of metabolic processes in mammalian cells (Meister, 1965) and, compared to normal tissues, certain cancer cells seem to function at low levels of L-glutamine availability because of slow rates of formation and rapid utilization (Holcenberg, Roberts & Dolowy, 1973). While L-asparaginase has little therapeutic effectiveness against human neoplasms other than lymphocytic leukemias (Clarkson, Krakoff, Burchenal, Karnofsky, Golbey, Dowling, Oettgen & Lipton, 1970), the permanent regression of Ehrlich carcinomas in rodents on treatment with bacterial glutaminase or glutaminase-asparaginases has been demonstrated (Roberts, Holcenberg & Dolowy, 1972), and a glutaminase-asparaginase from *Pseudomonas* 7A has been reported to have substantial activity against a variety of solid and ascites tumors in mice (Roberts, 1976; Roberts, Schmid & Rosenfeld, 1979). It would appear from these results that glutaminase treatment has the potential for human cancer therapy in malignancies other than leukemia.

The bacterial amidohydrolases are tetramers with molecular weights in the range of 120 000–147 000 g mol^{-1} (Wriston & Yellin, 1973). The amino acid sequence of an *E. coli* asparaginase revealed a 321 residue subunit with a (calculated) molecular weight of 34 080 g mol^{-1} (Maita, Morokuma & Matsuda, 1974). The subunits in each of the enzymes are believed to be identical with, to our knowledge, only one possible exception, that of an L-asparaginase from *Serratia marcescens* (Whelan & Wriston, 1974).

We are investigating the crystal structures of glutaminase-asparaginases from *Pseudomonas* 7A and *Acinetobacter glutaminasificans* (abbreviated as PGA and AGA). The enzymes have similar kinetic properties but quite different physical properties and biological half-lives. For example, with glutamine and asparagine substrates, the K_m's range over 4·4–5·8 μM and the ratios of the specific activities (L-gln/L-asn) are 2·0 and 1·2, respectively (Holcenberg, 1981). By comparison, the asparagine K_m for *E. coli* asparaginase is 12 μM and the L-gln/L-asn ratio is 0·03. The molecular weights of PGA and AGA are virtually identical at 138 000–139 000 g mol^{-1}, but the *pI*'s are 5·8 and 8·2. Substantial differences have been found in the sedimentation properties and plasma half-lives of the enzymes. Experiments with the glutaminase-asparaginase inhibitor 6-diazo-5-oxonorleucine (DON) have revealed a number of similarities between the enzymes and *E. coli* asparaginase (Holcenberg, Ericsson & Roberts, 1978). For example, the inhibitor bonds to a threonine located in identical 8 residue sections in the N-terminal regions of the two glutaminase-asparaginases, and an identical 8 amino acid fragment is present in the *E. coli* asparaginase. Half of the 60 residues in the N-terminal portions of the asparaginase and of AGA are identical.

Several of the amidohydrolases have been crystallized, and reports of preliminary crystallographic investigations have appeared since 1969. X-ray studies have provided evidence for molecular 222 point-group symmetry in the following enzymes: *E. coli* ATCC 9637 asparaginase (Epp, Steigemann, Formanek & Huber, 1971); *Proteus vulgaris* asparaginase (Lee, Yang, Henry & Seymour, 1975); *E. coli* HAP asparaginase (Itai, Yonei, Mitsui & Iitaka, 1976; Yonei, Mitsui & Iitaka, 1977). Exact 222 symmetry in the form III crystals of AGA was inferred from the space group $I222$ ($a = 96·7$, $b = 112·4$, $c = 70·9$ Å) with one subunit per asymmetric unit (Wlodawer, Roberts & Holcenberg, 1977). Although the 222 point group is compatible with either a square-planar or tetrahedral arrangement of subunits, the latter has been favored on the basis of molecular-packing criteria in several of these investigations. The structure of the *E. coli* HAP asparaginase at 5·8 Å has been the subject of a brief report (Mitsui, Satow, Watanabe, Hirono, Yonei, Urata, Torii & Iitaka, 1978), and we have recently obtained a 6 Å map of AGA (unpublished). The arrangement of subunits can be described as something between the limiting square-planar and tetrahedral structures.

PGA crystallizes in the orthorhombic space group $P2_12_12_1$ ($a = 118·0$, $b = 131·2$, $c = 85·1$ Å) with a full tetramer in the asymmetric unit. Unlike several of the asparaginases for which pseudo 222 symmetry was deduced, the PGA diffraction pattern does not reveal additional systematic absences at low resolution leading to a 'different' space group consistent with the presence of additional molecular symmetry. It is our plan to solve the single subunit structure of the *Acinetobacter* enzyme with the standard MIR methodology, after which molecular-replacement techniques (Rossmann, 1972; Argos & Rossmann, 1980) will be applied to the *Pseudomonas* 7A glutaminase-asparaginase problem. In this paper, we report the results of Patterson rotation studies of the symmetry of the PGA tetramer, and of

the relative orientations in the crystal of the *Pseudomonas* and *Acinetobacter* enzymes.

Experimental methods

AGA and PGA were purified to a homogeneous state as previously described (Roberts, Holcenberg & Dolowy, 1972; Roberts, 1976), and stored as lyophilized powders containing various amounts of phosphate. Crystallization was carried out with the basic recipes reported by Wlodawer, Roberts & Holcenberg (1977) with the hanging-drop, vapor-diffusion technique at 277 K. The PGA crystals formed as irregular diamond-shaped parallelepipeds with dimensions exceeding 2 mm in some cases. The AGA crystals grew as needles with rectangular cross-sections to a length of 0·8 mm, although most of the crystals were smaller. Crystals were trimmed where appropriate and mounted in siliconized glass capillaries.

Data collection

All data were collected on a PDP-8I computer-controlled Picker FACS-I diffractometer equipped with a highly oriented graphite-crystal monochromator, disc for program storage and magnetic-tape transport for data output. The original diffractometer configuration had been modified to utilize European standard sealed X-ray tubes and the detector arm was extended to provide a crystal to detector aperture distance of 51 cm. The diameters of the incident- and diffracted-beam 'collimators' were 1·0 and 1·5 mm, respectively, and an adjustable aperture at the detector was set to 3 × 3 mm. 33 cm of the diffracted-beam path length was through a helium-flushed tube. The X-ray source was a fine-focus Cu tube operated at 40 kV and 24 mA.

The PDP-8I software consisted of the Vanderbilt operating system (Lenhert, 1975). A stationary-detector-limited ω step-scan method (see Table 1) was used throughout for the intensity measurements. A reflection was rescanned over an adjusted range of ω if the step containing the maximum number of counts was displaced from the scan center by more than a specified amount (R_p, usually 1–3 steps). The number of steps the maximum count step was displaced from the center was printed as part of each reflection line, forming an effective visual trace of crystal misalignment. Friedel mates were measured at $\pm 2\theta$ in blocks of 25 reflections. Ten to fifteen standard reflections, depending on the crystal and data being measured, were collected at 200 reflection intervals.

Background data measurements were taken at selected empty regions of reciprocal space, and applied to each reflection with a modified version of the algorithm suggested by Krieger, Chambers, Christoph, Stroud & Trus (1974). A brief description of the scheme follows. Rotate φ at $\chi = 90°$ and $2\theta \simeq 25°$, and identify the angles corresponding to the minimum (φ_{min}) and maximum (φ_{max}) intensities; call this curve K_φ. Perform a 2θ step scan at 1° intervals over the range of data collection for the following φ, χ combinations: φ_{min}, $\chi = 90°$; φ_{max}, $\chi = 90°$; φ_{min}, $\chi = 0°$; φ_{max}, $\chi = 0°$. Call these curves *A*–*D*. Finally, record the χ (G_χ) dependence from 0–90° at φ_{min} and some intermediate value of 2θ. The background is calculated from the following equations:

$$F_\varphi = (K_\varphi - K_{\varphi_{min}})/(K_{\varphi_{max}} - K_{\varphi_{min}})$$

$$F_\chi = (G_\chi - G_{\chi=90°})/(G_{\chi=0°} - G_{\chi=90°})$$

$$A' = A_{\varphi_{min},\chi=90°}(1 - F_\varphi)$$

$$B' = B_{\varphi_{max},\chi=90°} F_\varphi$$

$$C' = C_{\varphi_{min},\chi=0°}(1 - F_\varphi)$$

$$D' = D_{\varphi_{max},\chi=0°} F_\varphi$$

$$\text{Background } (2\theta,\chi,\varphi) = (A' + B')(1 - G_\chi) + (C' + D')\,G_\chi.$$

Table 1. *Intensity-measurement information*

	Pseudomonas (four crystals)				
	1	2	3	4	*Acinetobacter*
Number of ω steps	9	9	9	7	9
Step time (s)	4	4	2	2	4
2θ range (°)	4–13·5	14·5–15·65	13·45–17·7	13·45–19	4–24
Maximum resolution (Å)	6·6	5·7	5·0	4·7	3·7
Total number of reflections	5709	4549[a]	4386[a]	5492[a]	9871
Number of unique reflections	2673	2223[a]	2078[a]	2636[a]	4336
Bijvoet *R* factor[b]	0·023	0·035	0·036	0·036	0·026
Mean intensity *R* factor[c]	0·022	0·029	0·029	0·032	0·025

(*a*) These numbers include a common set of reflections obtained for subsequent use in crystal-to-crystal scaling. The data set *hkl*'s were of the type $4n,2m,2r$ (n,m,r are integers), measured over $2\theta = 4$–14°. 230–250 data per crystal.

(*b*) $R = \sum |I_+ - I_-| / \sum (I_+ + I_-)$.

(*c*) $R = \sum_i \sum_j |I_{ij} - \langle I_i \rangle| / \sum_i \sum_j I_{ij}$, where $\langle I_i \rangle$ is the average value of the j measurements (I_{ij}) of the ith reflection.

Transmission curves for several reflections close to $\chi = 90°$ were measured, smoothed and averaged for use in absorption corrections (North, Phillips & Mathews, 1968).

Four crystals were used to measure the PGA data to $2\theta = 19°$ (4·7 Å), and one was used for AGA to $2\theta = 24°$ (3·7 Å) (see Table 1).

Integrated intensity determination

The ω step-scan data were fit to a Gaussian profile of the form:

$$I_i = C_1 \exp[-(\omega_i - C_2)^2/C_3^2],$$

where C_1 is the peak height, C_2 is the peak location, C_3 is proportional to the width and I_i and ω_i are the count and angle values for the ith step (Hanson, Watenpaugh, Sieker & Jensen, 1979). The profile fitting is a two-step procedure. In the first pass, all reflections for which at least six step intensities are $\geq 3\sigma$ above background are processed to give C_1, C_2 and C_3; the collection of C_3 values is used to parameterize a seven-term equation expressing C_3 as a function of h, k, l and θ. Separate width functions are determined for the reflections measured at $\pm 2\theta$. Integrated intensities are obtained for all reflections in a second pass, during which individual profiles are now fit to those scans having at least five step counts $> 3\sigma$. For those data which fail this cut, but which have at least three background-corrected step intensities ≥ 3 counts, the calculated C_3's (from the first-pass-determined parameters) are used to determine the peak centers, C_2's. For those reflections which fall below the three steps ≥ 3 count threshold, C_2 is obtained from the step with the highest intensity. If the peak center (C_2) is further from the middle of the step-scan range than the rescan parameter (R_p) × 0·04° (the angle increment per step), the reflection is eliminated from the data set. The C_2 and C_3 data for the surviving reflection are then used to obtain C_1 from:

$$C_1 = \sum_i I_i^{obs} I_i / \sum_i I_i^2,$$

where I_i^{obs} is the background-corrected intensity for the ith step. The integrated intensity is proportional to $C_1 C_3$. Two intensity estimates are obtained for the strongest reflections, one from a pass 1 type of profile fit and the other from the calculated C_3 value, and averaged for the final intensity value.

Radiation-damage corrections

The standard intensity data were used to determine the parameters for the crystal radiation-damage correction equation shown below. The equation is similar to one proposed by Hendrickson (1976), but uses an exponential term in the form of an anisotropic temperature factor:

$$I_0 = RI_t$$

$$R = A_1(t) + A_2(t) \exp[-2\pi^2(U_{11} h^2 a^{*2} + U_{22} k^2 b^{*2} + U_{33} l^2 c^{*2} + U_{12} hka^* b^* + U_{13} hla^* c^* + U_{23} klb^* c^*)].$$

I_0 is the intensity corrected to time 0, I_t is the observed value at time t, and A_1 and A_2 are constants which describe the basic shape and exponential dependence of the I_t *vs* t curves. Six values each for A_1 and A_2, usually equally spaced along the time axis, were used. The form of the exponential was required to correct for different rates of intensity decline in reflections with similar $\sin\theta/\lambda$ values. The six A_1's, A_2's and U_{ij}'s were determined by least squares. The standard reflection residuals, defined as

$$\text{Residual} = [\sum |(I_t/I_0^{obs}) - R|]/\sum (I_t/I_0^{obs}),$$

where I_0^{obs} is the 'observed' zero-time intensity, ranged from 0·01–0·04. The I_0^{obs} values were initially obtained from the first five intensity measurements of a particular standard extrapolated to $t = 0$, and later as the values required to minimize the I_t/I_0^{obs} *vs* R differences. This I_0^{obs} redetermination was followed by a final round of A_1, A_2 and U_{ij} determination.†

Computer programs

The majority of the standard crystallographic calculations were performed at the University of Maryland's Computer Science Center on Univac 1108 and 1100/42 computers with the XRAY system of programs (Stewart, Machin, Dickinson, Ammon, Heck & Flack, 1976). Additionally, a number of stand-alone programs, such as for decay corrections, crystal-to-crystal scaling, *etc.*, were used. The rotation-function calculations employed locally modified versions of the fast rotation function of Crowther (1972) and a program originated by Rossmann (Tollin & Rossmann, 1966). A number of the Rossmann-program calculations were carried out on a VAX 11/780 computer in the laboratory of D. R. Davies, National Institutes of Health, Bethesda, Maryland.

Results

The rotation function (R) is a measure of the overlap of two Patterson functions (P_1,P_2), following rotation of

† Lists of structure factors for the two enzymes have been deposited with the Protein Data Bank, Brookhaven National Laboratory (Reference: R1GAASF, R1GASSF), and are available in machine-readable form from the Protein Data Bank at Brookhaven or one of the affiliated centers at Cambridge, Melbourne or Osaka. The data have also been deposited with the British Library Lending Division as Supplementary Publication No. SUP 37008 (2 microfiche). Free copies may be obtained through The Executive Secretary, International Union of Crystallography, 5 Abbey Square, Chester CH1 2HU, England.

one (P_2) of them. The Crowther fast rotation function, which uses spherical harmonics, can handle a large portion of the available data and is relatively inexpensive to run. Our version of the program is based on the Eulerian angles α, β, and γ, is limited to a Patterson radius of 30 Å at 4·7 Å resolution and, for the $P2_12_12_1$ and $I222$ space groups of interest here, limits the α and γ grid to 2·5° and β to 5°. The Rossmann program performs a point-by-point rotation of the P_2 data set, and is substantially slower so that in practice only a limited quantity of the available P_2 data can be used. However, rotations can be made in spherical polar angles, κ, ψ, θ, or Eulerian angles, θ_1, θ_2, θ_3, and there is complete flexibility in regard to the radius of integration and angle search increment.

The 4·7 Å PGA and 6·0 Å AGA data were placed on an absolute scale with the XRAY system's scaling subprogram. This link operates with normalized structure factors, E_h, and produces scale and overall isotropic temperature factors on the basis of an average value for E_h^2 of 1·0. Because of this property, a sharpened, origin-free Patterson map can be calculated with $E_h^2 - 1$ as the Fourier summation coefficients.

The PGA and AGA Patterson functions have *mmm* symmetry, which results in both the 'self' and 'cross' rotation functions having the same space group, *Pbmb* (Rao, Jih & Hartsuck, 1980). The asymmetric units of the rotation maps in Eulerian angles are α = β = 0–90°, γ = 0–180°.

Pseudomonas 7A glutaminase-asparaginase self-rotation function

The three-dimensional self-rotation function for PGA was calculated with the fast rotation method using 10–4·7 Å data and a radius of integration of 30 Å. The rotation (R) maps were processed to subtract the average map value from each point, and scaled to make a value of 10 correspond to 1σ of the average. Several maps were calculated, with different amounts of data and E_h^2 *vs* $E_h^2 - 1$ coefficients. The resolution and definition in the $E_h^2 - 1$ map calculated with all of the data (6319 terms) were slightly superior to the others; these results are discussed in detail below.

Other than density associated with the origin regions, the asymmetric unit of the R map contained three peaks (Nos. 1–3) of about equal height located in general positions, plus two somewhat smaller peaks (Nos. [4,5] and 8) and a ripple (No. [6,7]). The [4,5], [6,7] and 8 maxima were all located on symmetry elements in the rotation map (Table 2). The relationships between these peaks with respect to possible pseudosymmetry in the PGA Patterson map was explored by transformation of the Eulerian angles to spherical polar angles which showed the rotational symmetries of the solutions. It is useful to think about the polar angle system (κ,ψ,φ) in terms of positioning the Patterson P_2 by the ψ and φ rotations, followed by a rotation of κ about the ψ, φ vector (Rossmann & Blow, 1962). In a few cases, it was necessary to transform the Eulerian angles to equivalent positions in the rotation-function space group, before conversion to polar angles, to reveal κ values close to 180°. In addition, the angle relationships between the various ψ, φ vectors were clarified by transformation to other equivalent positions which aided in the search for the expected orthogonality. The appropriately transformed κ, ψ, φ values are listed in Table 2, and the angles between the ψ, φ vectors corresponding to peaks 1–3 are given in Table 3. These data are further discussed below.

A similar investigation was carried out with the Rossmann program. Because of the large amounts of computer time required by the method, these studies were performed in spherical polar angles with κ fixed at 180° and with a limited number of terms from the P_2 data set. The P_1 data set contained all of the terms within the selected resolution limits and E_h^2's coefficients were used. The ψ, φ grid was usually 2° or 5°, with restricted range searches being conducted at 0·5° or 1·0° in the region of maxima. Again, several R maps were calculated with different radii of integration, resolutions and numbers of terms. The map used to produce the stereogram illustrated in Fig. 1 was calculated with 10–4·7 Å data, 25 Å radius of integration, 6319 P_1 terms and 994 P_2 terms. The peaks have been labeled to correspond to the fast rotation function maxima listed in Table 2. Peaks 1–3 are in general positions, 4–8 lie on mirror planes and the pairs [4,5] and [6,7] are related by φ = 0 and 90° axial symmetry.

Table 2. *Locations of the three fast rotation function peaks for Pseudomonas at* 10–4·7 Å *resolution*

	Eulerian angles (°)			Spherical polar angles (°)			
Peak	α	β	γ	κ	ψ	φ	Height[a]
Origin							11·2
1	6·5	87·0	173·5	180·0	85·5	−46·7	3·1
2	11·5	83·5	11·5	180·0	81·4	−137·7	3·3
3	87·0	17·0	87·5	180·1	8·9	72·7	3·2
[4,5][b]	90·0	26·0	90·0	180·0	13·0	90·0	2·3
[6,7][b,c]	52·0	0·0	90·0	180·0	19·0	0·0	2·4
8	0·0	90·0	0·0	180·0	90·0	45·0	2·3

(*a*) Peak height (n) expressed as $n\sigma$ above the average value.
(*b*) The double numbering is for convenience in referring to the κ = 180° Rossmann rotation function stereogram (Fig. 1).
(*c*) Ripple. Ripples of constant intensity, positioned such that α + γ is constant, are characteristic features of the β = 180° sections.

Table 3. *Angles between the transformed fast rotation function peaks*

Peak i	Peak j	
1	2	90·3°
1	3	89·8
2	3	89·1

An attempt was made to verify that $\kappa = 180°$ was the optimum value by calculating the Rossmann function with the same data and parameters, but with $\kappa = 178$, 179, 181 and 182°. These maps had all of the general features of the $\kappa = 180°$ maps, but in no case was a peak height larger than the corresponding one found at 180°.

Peaks 1–8 correspond to the following four sets of mutually orthogonal twofold rotation axes: (1) peaks 1–3 (see Tables 3 and 4); (2) peak 4, peak 5 transformed by $180° - \psi, \varphi$ and the crystallographic *a* axis; (3) peak 6, peak 7 transformed by $180° - \psi, \varphi$ and the *c* axis; (4) peak 8, peak 8 transformed by $\psi, -\varphi$ and the *b* axis. In the Rossmann function, the peak heights for 2–8 are about equal with peak 1 somewhat lower than the others, while in the fast rotation function, the heights of peaks 1–3 are about equal and *ca* 25% higher than the others. Taken at face value, the various peak heights in the Rossmann and fast rotation functions do not provide any clear indication as to which of these sets of axes represents the correct solution. However, it is important to realize that peaks 4–8 occur on symmetry elements, resulting in a doubling of their inherent magnitudes, and thus these peak heights should be halved when comparing them with other possible solution peaks. In the fast rotation function, for example, the ½ peak heights of [4,5] = 1·1, [6,7] = 1·1 and 8 = 1·2 should be compared with the values for peaks 1–3 of 3·1–3·3. This demonstrates that peaks 1–3 are substantially larger than 4–8 and, therefore, it is probable that they arise from the molecular symmetry of the PGA tetramer.

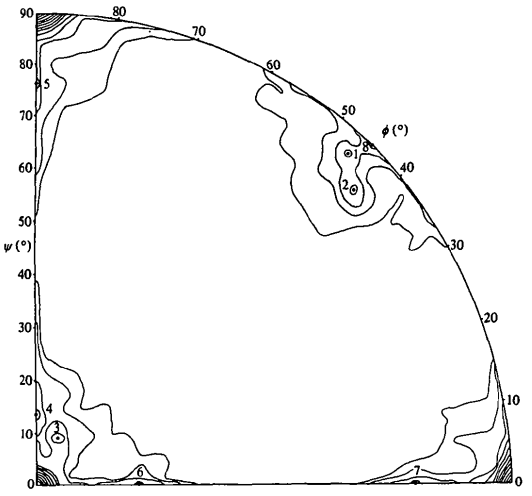

Fig. 1. A stereogram of the unique octant of the $\kappa = 180°$ rotation function for PGA. The crystallographic *a* axis is horizontal, *c* is vertical and *b* is at the center. The full stereogram has *mmm* symmetry. The conversions required to convert the ψ, φ values for peaks 1–3 to those reported in Table 5 are: (1) $\psi, -\varphi$; (2) $\psi, -180° + \varphi$; (3) ψ, φ.

Table 4. *Locations and angular relationships of the three peaks from the* $\kappa = 180°$ *Rossmann rotation functions*

Peak	ψ	φ	Height[a]	Peak *i*	Peak *j*	Angle
Origin			7·5			
1	85·8°	−46·7°	1·5	1	2	90·3°
2	81·8	−137·6	1·2	1	3	89·6
3	9·6	66·5	1·6	2	3	90·6
4	13·0	90·0	1·5			
5	77·0	90·0	1·5			
6	19·0	0·0	1·5			
7	71·0	0·0	1·5			
8	90·0	45·0	1·5			

(*a*) Peak height (*n*) expressed as $n\sigma$ above the average value.

Pseudomonas 7A vs Acinetobacter glutaminase-asparaginase cross-rotation function

The relative orientations of the two glutaminase-asparaginase structures were established with the so-called locked and cross-rotation functions. The locked function (Rossmann, Ford, Watson & Banaszak, 1972) compares two Patterson functions in a manner which should produce only those peaks that are consistent with all of the molecular symmetry. In the present investigation, the problem basically consisted of matching the (nonidentical) AGA twofold axes with the appropriate PGA axes. The twofold axes in AGA (P_2) are the crystallographic axes *a*, *b* and *c*, whereas in PGA (P_1), the pseudo twofold axes were derived from the fast rotation function peaks 1–3 (Table 2) by the $x = \sin\psi\cos\varphi$, $y = \cos\psi$, $z = -\sin\psi\sin\varphi$ transformation. The calculations can be thought of in terms of the superposition ('locking') of a P_2 axis to a P_1 axis, followed by the rotation (κ) of P_2 about the axis and the recording of the $P_1 \ldots P_2$ overlap as a function of the rotation angle. A total of nine combinations are possible: *viz a* locked to the peak 1

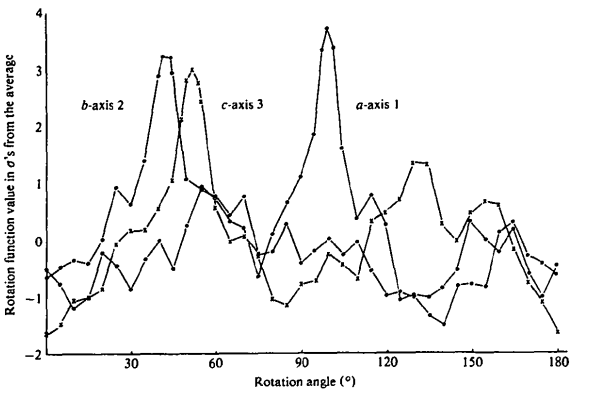

Fig. 2. Cross-rotation function searches for AGA *vs* PGA. *a*, *b*, and *c* refer to the crystallographic axes in AGA, whereas axes 1–3 refer to axes obtained from the PGA fast rotation maxima listed in Table 3.

Table 5. *Eulerian angles from the Acinetobacter vs Pseudomonas locked rotation function maxima*

R line	α	β	γ	Height[a]
a vs peak 1	87·0°	99·0°	42·7°	3·72
b vs peak 2	87·1	99·6	42·5	3·23
c vs peak 3	87·3	98·5	40·8	3·01

(*a*) Peak height (*n*) expressed as $n\sigma$ above the average value.

Table 6. *Eulerian angles from the three-dimensional AGA vs PGA rotation functions*

R map	α	β	γ
Fast rotation function	86·1°	98·5°	42·0°
Rossmann function	86·4	98·5	42·4

axis, *b* locked to the peak 1 axis, *c* locked to the peak 1 axis, *etc.* The nine *R* maps (lines) should contain only three maxima, corresponding to the optimum pairing of each of the P_2 axes with a different one of the P_1 axes, and provide a threefold redundancy of information on the relative orientation of the two Patterson functions. That is, the overall rotation of P_2 deduced from a maximum on the *R* line with, say, the P_2 *a* axis locked to the P_1 peak 1 axis, should be the same as that calculated from the two other *R*-line maxima.

In the interest of conserving computer time, only 'large term' calculations were performed for all nine combinations. The following parameters proved adequate: 10–6 Å resolution; 50 Å radius of integration; P_1, 284 $E_h^2 > 2{\cdot}0$; P_2, 57 $E_h^2 > 2{\cdot}0$; $\kappa = 0$–180° search in 5° steps, 1° steps at the peak locations. In fact, the use of more data only served to decrease the *R*-line peak/background ratios. Three *R*-line peaks, 3–3·7σ above the average line values, were observed. The lines are illustrated in Fig. 2, and the peak locations, converted to the fast rotation function, Eulerian angles are listed in Table 5. Similar sets of 'locked' calculations, performed with the solutions derived from peaks [4,5], [6,7] and 8 in the self-rotation maps, gave extremely noisy *R* lines with no indication of an alternative valid solution.

The full three-dimensional cross-rotation function was calculated with the fast rotation program, 10–4·7 Å data, a radius of integration of 30 Å, and the following set of coefficients: PGA, P_1, 1206 $E_h^2 > 1{\cdot}6$; AGA, P_2, 666 $E_h^2 > 0{\cdot}8$. The map contained only a single peak 6–7σ above background. A Rossmann-program calculation was carried out with a 1° Eulerian angle grid around the fast rotation function maximum. These positions are reported in Table 6.

Discussion

The noncrystallographic symmetry of the *Pseudomonas* 7A glutaminase-asparaginase Patterson function has been investigated with rotation function techniques, utilizing both the Crowther spherical harmonics and Rossmann algorithms. The fast rotation function map contains only three peaks of about the same height plus two prominent ripples on the $\beta = 0°$ section, one of which is the characteristic origin ripple. The Rossmann-function section at $\kappa = 180°$ consists of four distinct peaks, of which three correspond to the three fast rotation function peaks and one to the $\beta = 0°$ ripple. The three peaks correspond to twofold rotations about orthogonal axes, leading to the interpretation that the PGA tetramer has 222 point-group symmetry.

Two previous rotation-function studies, those of the *E. coli* (Epp, Steigemann, Formanek & Huber, 1971) and *Proteus vulgaris* (Lee, Yang, Henry & Seymour, 1975) asparaginases, have been interpreted in terms of pseudo 222 symmetry. In both cases, however, the reciprocal lattices contained additional systematic absences at low resolution (≥ 10 Å) which were consistent with 'new' space groups and tetramer symmetries. At low resolution, the space group of the *E. coli* enzyme changed from $C2$ to $I222$, while the *Proteus* asparaginase space group went from $P2_1$ to $A2$. Subsequent Patterson rotation studies confirmed the presence of pseudo 222 point-group symmetry in both structures. Our present investigation of the *Pseudomonas* 7A enzyme is the first of the amidohydrolases which does not show additional symmetry at low resolution, but for which 222 symmetry has been determined.

The relative orientations of the *Acinetobacter* and *Pseudomonas* glutaminase-asparaginase Patterson functions were determined with the locked and three-dimensional rotation methods. This is equivalent to determining the orientations of the two tetrameric enzyme molecules, the first of which has exact, crystallographic 222 symmetry while the second has pseudo symmetry. Since the AGA crystals contain one subunit per asymmetric unit and the PGA one tetramer (four subunits) per asymmetric unit, it might be thought that the cross-rotation functions should contain four peaks, one for each 'hit' of the AGA subunit with a different PGA subunit. However, it must be realized that it is the AGA Patterson function with 222 symmetry that is being rotated against the PGA Patterson function, and thus there will be only a single orientation which produces simultaneous overlap of all elements of the AGA 222 point group with the PGA 'noncrystallographic' 222 point group. If, however, an AGA subunit model had been used to calculate a Patterson function with only $\bar{1}$ point-group symmetry, then four 'hits' would be expected by rotation against the PGA Patterson function.

We presently are carrying out heavy-atom soaking experiments for the *Pseudomonas* enzyme, and these rotation-function results will be of substantial value in locating the heavy atoms in Patterson difference maps.

Additionally, the cross-rotation function results represent the first step toward utilizing the AGA subunit structure to solve the PGA tetramer structure. A solution to the PGA translation problem will be explored with the use of the AGA structure and translation function techniques (*e.g.* Harada, Lifchitz, Berthou & Jolles, 1981), and by a direct interpretation of a PGA heavy-atom difference Patterson map to determine a molecular center (Argos & Rossmann, 1974).

This work was supported by the National Science Foundation (grant No. PCM-79-07501) and, in part, through the facilities of the University of Maryland's Computer Science Center. Our thanks to Dr D. R. Davies for his hospitality to HLA, and for the use of the Vax 11/780 computer.

References

ARGOS, P. & ROSSMANN, M. G. (1974). *Acta Cryst.* A**30**, 672–677.

ARGOS, P. & ROSSMANN, M. G. (1980). *Theory and Practice of Direct Methods in Crystallography*, edited by M. F. C. LADD & R. A. PALMER, pp. 361–417. New York: Plenum.

CLARKSON, B., KRAKOFF, I., BURCHENAL, J., KARNOFSKY, D., GOLBEY, R., DOWLING, M., OETTGEN, H. & LIPTON, A. (1970). *Cancer*, **25**, 279–305.

COONEY, D. A., DRISCOL, J. S., MILMAN, H. A., JAYARAM, H. N. & DAVIS, R. D. (1976). *Cancer Treat. Rep.* **60**, 1493–1557.

CROWTHER, R. A. (1972). *The Molecular Replacement Method*, edited by M. G. ROSSMANN, pp. 173–178. New York: Gordon and Breach.

EPP, O., STEIGEMANN, W., FORMANEK, H. & HUBER, R. (1971). *Eur. J. Biochem.* **20**, 432–437.

HANSON, J. C., WATENPAUGH, K. D., SIEKER, L. & JENSEN, L. H. (1979). *Acta Cryst.* A**35**, 616–621.

HARADA, Y., LIFCHITZ, A., BERTHOU, J. & JOLLES, P. (1981). *Acta Cryst.* A**37**, 398–406.

HENDRICKSON, W. A. (1976). *J. Mol. Biol.* **106**, 889–893.

HOLCENBERG, J. S. (1981). Editor, *Enzymes as Drugs*, pp. 25–61. New York: John Wiley.

HOLCENBERG, J. S., ERICSSON, L. & ROBERTS, J. (1978). *Biochemistry*, **17**, 411–417.

HOLCENBERG, J. S., ROBERTS, J. & DOLOWY, W. C. (1973). *The Enzymes of Glutamine Metabolism*, edited by A. PRUSINER & E. R. STADTMAN, pp. 277–292. New York: Academic Press.

ITAI, A., YONEI, M., MITSUI, Y. & IITAKA, Y. (1976). *J. Mol. Biol.* **105**, 321–325.

KIDD, J. G. (1970). *Recent Results Cancer Res.* **33**, 3–14.

KRIEGER, M., CHAMBERS, J. L., CHRISTOPH, G. G., STROUD, R. M. & TRUS, B. L. (1974). *Acta Cryst.* A**30**, 740–748.

LEE, B., YANG, H. J., HENRY, G. M. & SEYMOUR, J. P. (1975). *J. Biol. Chem.* **250**, 6228–6231.

LENHERT, P. G. (1975). *J. Appl. Cryst.* **8**, 568–570.

MAITA, T., MOROKUMA, K. & MATSUDA, G. (1974). *J. Biochem.* **76**, 1351–1354.

MEISTER, A. (1965). *Biochemistry of the Amino Acids*, Vol. 2, 2nd ed., pp. 617–636. New York: Academic Press.

MITSUI, Y., SATOW, Y., WATANABE, Y., HIRONO, S., YONEI, M., URATA, Y., TORII, K. & IITAKA, Y. (1978). *Acta Cryst.* A**34**, S60.

MONTGOMERY, J. A. (1976). *Prog. Drug Res.* **20**, 465–490.

NORTH, A. T. C., PHILLIPS, D. C. & MATHEWS, F. S. (1968). *Acta Cryst.* A**24**, 351–359.

OETTGEN, H. F., OLD, L. J., BOYSE, E. A., CAMPBELL, H. A., PHILIPS, F. S., CLARKSON, B. D., TALLAL, L., LEEPER, R. D., SCHWARTZ, M. K. & KIM, J. H. (1969). *Cancer Res.* **27**, 2619–2631.

RAO, S. N., JIH, J. & HARTSUCK, J. A. (1980). *Acta Cryst.* A**36**, 878–884.

ROBERTS, J. (1976). *J. Biol. Chem.* **251**, 2119–2123.

ROBERTS, J., HOLCENBERG, J. S. & DOLOWY, W. C. (1972). *J. Biol. Chem.* **247**, 84–90.

ROBERTS, J., SCHMID, F. A. & ROSENFELD, H. J. (1979). *Cancer Treat. Rep.* **63**, 1045–1054.

ROSSMANN, M. G. (1972). *The Molecular Replacement Method, a Collection of Papers on the Use of Non-Crystallographic Symmetry*. New York: Gordon and Breach.

ROSSMANN, M. G. & BLOW, D. M. (1962). *Acta Cryst.* **15**, 24–31.

ROSSMANN, M. G., FORD, G. C., WATSON, H. C. & BANASZAK, L. J. (1972). *J. Mol. Biol.* **64**, 237–249.

STEWART, J.M., MACHIN, P. A., DICKINSON, C. W., AMMON, H. L., HECK, H. & FLACK, H. (1976). The XRAY system. Tech. Rep. TR-446. Computer Science Center, College Park, Univ. of Maryland.

TOLLIN, P. G. & ROSSMANN, M. G. (1966). *Acta Cryst.* **21**, 872–876.

WHELAN, H. A. & WRISTON, J. C. (1974). *Biochim. Biophys. Acta*, **365**, 212–222.

WLODAWER, A., ROBERTS, J. & HOLCENBERG, J. S. (1977). *J. Mol. Biol.* **112**, 515–519.

WRISTON, J. C. & YELLIN, T. O. (1973). *Advances in Enzymology*, Vol. 39, edited by A. MEISTER, pp. 185–248. New York: John Wiley.

YONEI, M., MITSUI, Y. & IITAKA, Y. (1977). *J. Mol. Biol.* **110**, 179–186.